Journal of Quantitative Spectroscopy & Radiative Transfer 224 (2019) 176–184

Contents lists available at ScienceDirect

Journal of Quantitative Spectroscopy & Radiative Transfer

journal homepage: www.elsevier.com/locate/jqsrt

Dynamic spatial fusion of cloud top phase from PARASOL, CALIPSO, cloudsat satellite data

Zhenting Chen[a,b,c], Xiaobing Sun[b,*]

[a] Kunming University, Institute of Information Technology, Kunming, Yunnan, China
[b] Key Laboratory of Optical Calibration and Characterization, Anhui Institute of Optics and Fine Mechanics, Chinese Academy of Sciences, Hefei, China
[c] University of Science and Technology of China, Hefei, Anhui 230026

ARTICLE INFO

Article history:
Received 20 March 2018
Revised 4 November 2018
Accepted 5 November 2018
Available online 7 November 2018

Keywords:
Cloud phase
Polder3
Calipso
Cloudsat
Modis
Spatial fusion

ABSTRACT

Cloud phase is one of the important parameters of weather and climate research and core elements of atmospheric cloud parametric inversion. The accuracy of its recognition directly influences the inversion precision of cloud optical thickness, spherical albedo, effective particle radius, ice/liquid water content and other parameters. In this paper, we combine with cloud phase products of spaceborne multi-angle polarimetric radiometer, polarized laser radar, and millimeter wave radar. Next, we put forward a Dynamic Spatial Optimal Fusion (DSOF) algorithm. In this algorithm we construct the spatial optimal fusion rules of Cloud Top Phase (CTP) for multi-source data. Finally, we realize the cloud phase spatial fusion using these rules. We used the typhoon "Lupit" as the research object and verified this method. The standard deviations are 4.67%, 7.18%, 40.14% and 36.51%, respectively, compared the results of fused CTP to that of CALIPSO, CloudSat, POLDER3 and MODIS. The fusion results are most close to the CTP of CALIPSO. The results show that this method can effectively achieve multi-source cloud phase inversion, and provide new technology for the development and data synergy of spaceborne multi-sensor satellite.

1. Introduction

Clouds are the key factor influencing global weather and climate change and play a very important role in atmospheric energy exchange, earth radiation budget an d hydrological cycle [1,2]. The study of cloud macrophysical, microphysical, and optical properties and their spatial-temporal variations will help to improve and enhance the atmospheric circulation and weather prediction model [3]. Cloud phase usually refers to the thermodynamic form of cloud particles (ice/water phase). The scattering and absorption procedure of cloud particles are clearly different under various physical states, and the phase change is accompanied by the complicated thermodynamic transformational process. As a core parameter of clouds, the accurate identification of cloud phase can not only help to realize the inversion of other cloud microphysical characteristics but also enhance the understanding of global weather system evolution. In addition, the aircraft is easy to freeze through supercool clouds. The icing accumulation will change the aerodynamic performance of aircraft and affect the flight safety. However, cloud phase is conducive to accurately determine supercool clouds, and reduce the risk of icing. In the field of weather and meteorological prediction, cloud phase can improve the initial field of corresponding numerical models, and also can check and correct the predicting results. Furthermore, it is helpful for determining the coverage area of clouds, fog, and precipitation, and enhance the accurate understanding and prediction of weather and climate change rules.

With the development of satellite remote sensing technology, many advanced sensors had been launched. These sensors enriched the data sources to study the changing process of cloud physics from the global scale. According to the different way of emitting and receiving energy, remote sensing technology is usually divided into passive and active method. In recent decades, many scholars had proposed a variety of cloud phase inversion methods for different satellite sensors [4–7]. Ackerman et al. [8] studied the optical properties of cirrus using airborne High-spectral resolution Interferometer Sounder (HIS) instrument and ground laser radar, and first proposed a trispectral method of cloud phase inversion based on thermal infrared (8, 11, 12 μm) band. Strabala et al. [9] further studied trispectral method using airborne MODerate resolution Imaging Spectroradiometer (MODIS) instrument and found the ice and water clouds can accurately be distinguished in 8.5, 11 and 12 μm channels, but it is easy to misjudge the phase of thin clouds. Baum et al. [10] presented a bispectrum cloud phase operational algorithm based on airborne MODIS data and used the brightness temperature difference between the 8.5 and 11 μm channel to

* Corresponding author.
E-mail address: xbsun@aiofm.ac.cn (X. Sun).

https://doi.org/10.1016/j.jqsrt.2018.11.010
0022-4073/

identify the cloud phase. In the International Satellite Cloud Climatology Project (ISCCP), Rossow et al. [11] identify the cloud phase by the 11 μm brightness temperature difference of the Advanced Very High Resolution Radiometer (AVHRR) sensor data. King et al. [12] compared the near-infrared (1.6, 2.1 μm) reflectivity and visible (0.66 μm) channel of spaceborne MODIS, and achieved recognition of cloud phase by ratio threshold method, but it is difficult to thin cirrus. A large number of aeronautical polarization experiments have found that cloud particles show different polarized radiative characteristics with different scattering angle. The liquid droplets show the main polarized rainbow near the 140° scattering angle [1,13]. On the contrary, the polarized radiation of ice particles decreases with scattering angle increasing. Goloub et al. [13] proposed the operational cloud phase recognition algorithm of POLarization and Directionality of the Earth's Reflectances (POLDER) using the polarized characteristics of clouds. Furthermore, he found a good consistency compared with ground-based lidar measurements. However, when the cirrus optical thickness is less than 2, the cirrus above the multilayer clouds will be misclassified as water clouds. Riédi et al. [14] combined three different methods (POLDER polarization algorithm, MODIS thermal infrared bispectral algorithm and MODIS shortwave infrared bispectral algorithm) to realize synergetic inversion of CTP. He replaced the traditional discrete classification (liquid, ice, and mixed phase) to a semi-continuous index. This method is expected to be conducive to the assimilation and modeling of global cloud properties derived from satellite data.

Spaceborne active remote sensing mainly includes laser and microwave detecting ways. The National Aeronautics and Space Administration (NASA) had launched the Cloud-Aerosol Lidar and Infrared Pathfinder Satellite Observation (CALIPSO) and CloudSat satellite, which carrying Cloud-Aerosol Lidar with Orthogonal Polarization (CALIOP) and Cloud Profile Radar (CPR) sensors respectively. These sensors are used for synergistic cloud observation. Hu et al. [15] improved the depolarization ratio algorithm using CALIOP data. He recognized particle random oriented ice clouds, horizontal oriented ice clouds and water clouds using a 2-dimensional (2-D) threshold. Then he separated water clouds from particle horizontal oriented ice clouds by using the spatial correlation technology. Wang et al. [16] presented operational cloud phase identification of CloudSat combined with CALIPSO data. It is accurate to precipitation cloud detection and effective to the top of thin clouds and multilayer clouds. Cho et al. [17] compared MODIS infrared cloud phase information with CALIOP product. It shows that most of the opaque middle-temperature clouds are divided into unknown or mixed phase. However, it is invalid for transparent clouds.

The cloud phase inversion of single sensor has its own limitations restricted by the single performance of the instrument. The multi-sensor synergistic inversion is mainly focused on horizontal or vertical directional combination. The combination of horizontal and vertical direction is relatively less on retrieving cloud phase from 3-dimensional (3-D) space. With the operation of "A-Train" satellites in orbit, it becomes possible to synergistic inversion of cloud phase based on multi-sensor detection information, and the inversion of cloud phase space cooperation can break through the traditional single recognition method, and collaborative processing with a variety of techniques. Furthermore, it can provides a new technology for atmospheric collaborative observation and retrieval, and provide new solutions for climate change, weather change, artificial intervention weather, extreme meteorological disaster prevention and aircraft flight safety. This paper carried out collaborative processing of horizontal and vertical direction based on the satellite polarization (POLDER), laser (CALIPSO) and microwave (CloudSat) data, and construct spatial synergistic inversion process and algorithm which will provide methods and technical support for synergistic inversion of cloud properties and future satellite space exploration.

The CALIOP, CPR, POLDER3, and MODIS sensors have their own characters with different transmitting and receiving energy. The main cloud phase inversion algorithms of different sensors are introduced. Section 2 discusses the main data characteristics of different instruments, and we have a brief introduction to the information of different operational products. A multidimensional DSOF algorithm is developed in Section 3. The spatial synergistic methods of cloud phase from horizontal and vertical direction are established with multi-objective fuzzy rules. The results and analysis are presented in Section 4. Discussion and conclusions are given in Section 5.

2. Data

2.1. POLDER3

France had launched the Polarization and Anisotropy of Reflectance for Atmospheric Science coupled with Observations from a Lidar (PARASOL) satellite in December 2004, loaded POLDER3, as a part of "A-Train" satellites. POLDER3 is multi-spectral, multi-directional and multi-polarized imaging radiometer [18]. When PARASOL passes over the objects, the radiometer can acquire 16 different images from visible and near-infrared spectral bands [19]. Compared to the ocean and land surface, the polarized characters of clouds and aerosols [20,21] are more sensitive to the observing angle. The polarized characters of clouds depend mainly on the shape and size of cloud particles. With the change of scattering angle the polarized reflectance of water clouds have an obvious increase called primary rainbow (140°) and the ice clouds have presented diminishing values. These features are used to discriminate the water clouds and ice clouds [22–24].

The French National Space Research Center (CNES) provides three level products. All products can be downloaded from the ICARE website (www.icare.univ-lille1.fr). The level 2 products is divided into three independent processes referred to as the land surfaces, the ocean, and the Radiation Budget (RB). The RB products obtained the parameters of cloud coverage area such as cloud phase, optical thickness, oxygen pressure, albedo, etc. The level 2 products use medium resolution grid which approximately equal to 3×3 POLDER pixels (Fig. 1). The data structure of level 2 is composed of four data domains and ancillary description. The cloud phase is stored in the 2-D table named cloud_phase. We know that the POLDER3 cloud phase index is coded with values ranging from 0 to 255 because the index is derived using various tests. The unobserved area is filled with 255, 254 indicate missing values, 240 indicate clear sky region, 230–239 indicate the undetermined region, 200–229 indicate mixed phase, 100–199 indicate ice phase, 0–99 indicate water phase.

2.2. CALIPSO

The CALIPSO had been launched on April 28, 2006, as a part of 'A-Train', equipped with the CALIOP sensor by NASA and the Centre National d'Études Spatiales (CNES). There are four level products such as Level 1B, Level 1.5, Level 2, and Level 3. The product parameters are radar depolarization ratio, aerosol optical thickness, cloud top height, backscattering coefficient, Vertical Feature Mask (VFM), cloud type, etc. The cloud phase recognition of CALIOP is realized by using the lidar linear depolarization ratios of clouds [25–27]. The cloud phase is stored in the VFM of Level 2 with HDF format. From the Atmospheric Science Data Center (ASDC) of NASA, we can get the CAL_LID_L2_VFM-ValStage1 data free (https://eosweb.larc.nasa.gov/order-data).

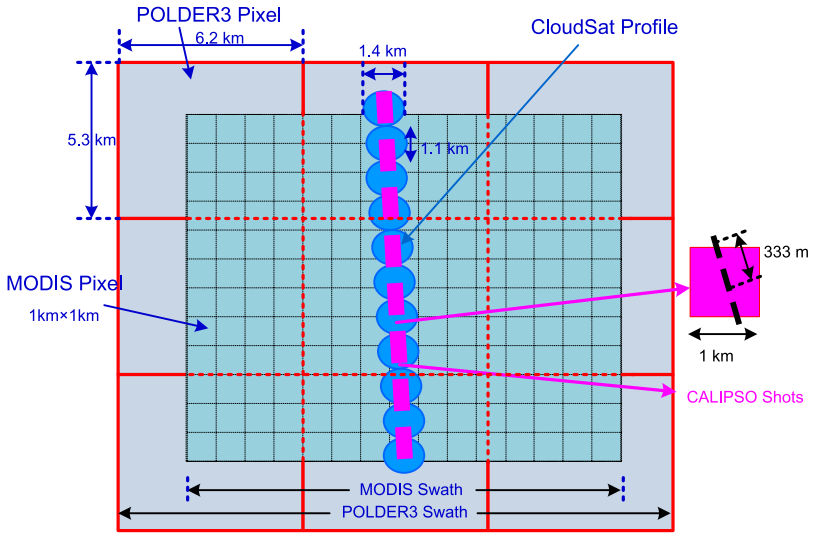

Fig. 1. Horizontal resolutions for POLDER3, MODIS, CloudSat and CALIPSO, where gray boxes represent $5.3 \times 6.2\,km^2$ POLDER3, $1 \times 1\,km^2$ boxes represent MODIS pixel, blue ellipses are 1.1 km CloudSat profiles, and purple dashed lines are CALIPSO shots with 333 m horizontal resolution.

The VFM product have the "Feature_Classification_Flags" parameter which stores a series of cloud and aerosol characteristic value composed of 16-bit unsigned integer. The effective range of value is 1–49,146. The different feature types are stored in different digits, 1–3 bit is stored feature types, 4–5 bit is stored quality of feature type, 6–7 bit is stored ice/water phase, 8–9 bit is stored quality of ice/water phase, 10–12 bit is stored feature subtype, 13 bit is stored quality of cloud/aerosol/polar stratospheric cloud type, 14–16 bit is stored mean of detecting horizontal resolution. The range of cloud phase value is 0–3, 0 is the unknown or not determined, 1 is ice phase, 2 is water phase, and 3 is mixed phase.

2.3. CloudSat

CloudSat was launched on a Delta II rocket with CALIPSO together. The main instrument on CloudSat is a Cloud Profiling Radar (CPR) of 94 GHz. The purpose of CloudSat mission is to measure vertical structure of clouds and observe precipitation. The experts of CloudSat Science team have developed the scientific algorithms and software tool for the CloudSat Products [28]. The Data Processing Center (DPC) will provide 18 types of standard products such as 1B-CPR, 2B-GEOPROF, 2B-FLXHR, 2B-CLDCLASS, 2B-CLDCLASS-LIDAR, etc. Now, all products can be downloaded from the University of Colorado's official website (www.cloudsat.cira.colostate.edu), and we get the 2B-CLDCLASS-LIDAR data from the CloudSat Data Process Center (DPC).

Although CALIPSO Level 2 products provides water or ice cloud feature, the backscatter signals of lidar are easily affected by multiple scattering [29] of cloud particles in multi-layer clouds. A reliable method combining CPR and CALIOP was developed to identify multi-layer cloud phase and can avoid the limitations of lidar. The 2B-CLDCLASS-LIDAR is produced by using the combined method. The cloud phase data is stored in a 3-D table. The effective range of CloudSat cloud phase values is marked from 0 to 3 with different cloud layer (0 is unknown or undetermined, 1 is the ice phase, 2 is the mixed phase, and 3 is the water phase).

2.4. MODIS

The MODIS sensors were launched by NASA in 1999 and 2002 loaded by the Terra and Aqua satellite respectively. The instruments can capture data in 36 spectral bands ranging in wavelength from 0.4 to 14.4 μm. It can provide cloud boundaries, cloud properties, ocean color, aerosols, surface temperatures, cloud phase, and other information. It can be used for long-term global observations of the Earth's surface, biosphere, solid earth, atmosphere, and oceans. The team of MODIS scientists is divided into 4 disciplines, the atmosphere, the land, the ocean and the calibration group. There are six Level 2 atmosphere products collected from two platforms (Terra and Aqua). The cloud products are assigned an 8-character data type named MOD06_L2 (Terra) and MYD06_L2 (Aqua). The MODIS cloud phase products can be downloaded from the Atmosphere Archive & Distribution System (LAADS) of NASA. At first, Strabala et al. [9] developed a trispectral infrared technique (8.5, 11, 12 μm) for cloud phase discrimination. Then this method was reduced to a bispectral technique (8.5, 11 μm) for MODIS in Collection5. The infrared phase was divided into four categories (water, ice, mixed phase, and undetermined). The range of numerical values is from 0 to 6 in MODIS cloud phase product, 0 is the cloud-free region, 1 is water clouds, 2 is ice clouds, 3 is mixed phase clouds, and 6 is the undetermined phase [7]. Some researchers have found transparent thin cirrus may not be identified as ice clouds in infrared band and supercooled water or mixed phase clouds will lose effectiveness in recent years [17,30]. The mixed and undetermined phase of MODIS are combined into uncertain phase in Collection 6.

3. Methods

There are diverse structures and dimensions from the polarization, laser, and microwave satellite data. The data of different dimensions need to be unified in the same dimensional space. In order to carry out the operation of ascending and reducing dimension, the following mathematical definitions need to be made according to the related theory of subspace and tensor algebra [31].In the n-dimensional (n-D) Euclidean space $\mathbb{R}^n$system, an arbitrary dimensional spatial vector can be converted to high or low dimensional spatial vector, the transformation process is called ascending dimension and reducing dimension, with the symbol $=\uparrow$ and $=\downarrow$, respectively.

We define: In the 2-D Euclidean space $\mathbb{R}^2$, if there is 2-D vector set {**A**, **B**, **C**}, there must be a 3-D vector **D** in 3-D Euclidean space $\mathbb{R}^3$, and meet $\mathbf{D} = \downarrow \boldsymbol{\alpha}\mathbf{A} + \boldsymbol{\beta}\mathbf{B} + \boldsymbol{\gamma}\mathbf{C} + \boldsymbol{\omega}$, where **A**, **B**, **C** are the same property dataset of three sensors, $\boldsymbol{\alpha}$, $\boldsymbol{\beta}$, $\boldsymbol{\gamma}$ are weight coefficients dataset, $\boldsymbol{\omega}$ is transformation constant.

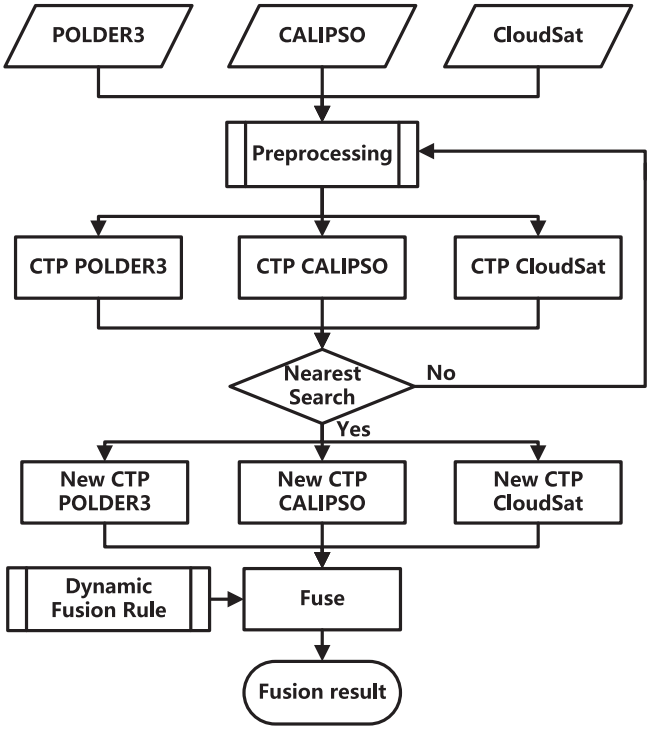

Fig. 2. Flow chart of the DSOF algorithm for cloud top phase.

The CALIPSO, CloudSat, PARASOL are sun-synchronous orbit satellites and have the same orbit height. The time interval is short to observe the same ground target, the characteristics of earth and atmospheric targets can be regarded as unchanged. We consider that three sensors (POLDER3, CALIOP, and CPR) are same linear space, so the data can be processed in spatial synergism.

We set up the spatial synergistic fusion rules of cloud phase from horizontal direction based on above consideration. The phase of cloud top is different from three sensors in the horizontal direction. Therefore, a DSOF algorithm is established in order to realize the cloud top phase fusion (Fig. 2).

We assume the cloud phase of three satellites (CALIPSO, CloudSat, and PARASOL) in 2-D space are $\mathbf{P}_A$, $\mathbf{P}_B$, $\mathbf{P}_C$, respectively. The fusion cloud phase in 3-D space is $\mathbf{D}_3$. it can be obtained by the following formula:

$$\mathbf{D}_3 = \downarrow \boldsymbol{\alpha}\mathbf{P}_A + \boldsymbol{\beta}\mathbf{P}_B + \boldsymbol{\gamma}\mathbf{P}_C + \varpi \tag{1}$$

where *A*, B, C are the sensors of CALIPSO, CloudSat, and PARASOL, respectively, $\boldsymbol{\alpha}$, $\boldsymbol{\beta}$, $\boldsymbol{\gamma}$ are weight coefficients of cloud phase of different sensor, ϖ is transformation constant.

We reduce the dimension of cloud phase by formula 1 with projection transformation, and the fusion CTP of three sensors in the 2-D space is expressed as $\mathbf{F}_{min}$ by replacing $\mathbf{D}_3$ in 3-D space. We select CALIPSO CTP with the highest resolution as the benchmark. Then we search the matching value by find the nearest location (latitude and longitude) in other two 2-D spatial cloud phase data, and get the new CloudSat and PARASOL CTP data.

$$\begin{cases} P_A = \mathbf{P_A} \\ P_B = \|\mathbf{P_B}\|_{nearest} \\ P_C = \|\mathbf{P_C}\|_{nearest} \end{cases} \tag{2}$$

From above operation, we get three sensor's CTP dataset $\{P_A, P_B, P_C\}$ in 2-D space under the same resolution. In order to realize the fusion of CTP, the dynamic fusion rule of multiple targets is established, which is defined as follows:

$$\begin{cases} F_{min} = aP_A + bP_B + cP_C + \varpi \\ a + b + c = 1 \\ 0 \le a \le 1, 0 \le b \le 1, 0 \le c \le 1, \varpi = 0 \end{cases} \tag{3}$$

where P_A, P_B, P_C are cloud phase inversion results of CALIPSO, CloudSat, and PARASOL, respectively. *a, b, c* are the weight coefficient's value of cloud phase of three sensors in the fusion process, and meet $a \in \boldsymbol{\alpha}$, $b \in \boldsymbol{\beta}$, $c \in \boldsymbol{\gamma}$.

Because the weight coefficient is dynamic, the fusion process is more complicated. The change of the coefficients will lead to certain differences in the results of the fused cloud phase. In order to optimize the dynamic fusion algorithm, we construct a spatial optimal fusion rules. The rules are established as followed:

(a) When $a=1$ and $b=c=0$, the fusion phase F_{min} only represents CALIPSO CTP from the formula 3. When $a=c=0$ and $b=1$, the fusion phase F_{min}only represents CloudSat CTP, while $a=b=0$ and $c=1$, the fusion phase F_{min} only represents PARASOL CTP;
(b) If $P_A=P_B=P_C$ and $a=b=c=1/3$, the fusion phase $F_{min}=aP_A+bP_B+cP_C=P_A$;
(c) If $P_A=P_B \neq P_C$ and $a=b=1/2$, $c=0$, the fusion phase $F_{min}=aP_A+bP_B=P_A$. Or, if $P_A \neq P_B=P_C$ and $b=c=1/2$, $a=0$, the fusion phase $F_{min}=bP_B+cP_C=P_B$. Or, if $P_A=P_C \neq P_B$ and $a=c=1/2$, $b=0$, the fusion phase $F_{min}=aP_A+cP_C=P_C$.
(d) If $P_A \neq P_B \neq P_C$ and *a, b, c* are arbitrary nonnegative real numbers ($a \in [0, 1]$, $b \in [0, 1]$, $c \in [0, 1]$), then the fusion results are computed by $F_{min}=aP_A+bP_B+cP_C$. When $\Delta F_{min} = Minimum(\| F_{min} - \bar{F} \|)$ is the optimal value ($\bar{F}$ is the average of cloud phase under different weighting coefficients), then the fusion phase is the optimal solution.

The fused output is the result of cloud top phase fusion$\{F_{min}\}$.

4. Results and analysis

We choose the No.20 tropical storm "Lupit" as the research object with its thicker and multi-layer cloud structure. It was generated in the early morning of October 16, 2009, in the western Pacific. In the following days, it gradually developed into a super typhoon. Four satellites (Aqua, CALIPSO, CloudSat, and PARASOL) were just passing over the typhoon "Lupit" and acquired the observing data in October 21. The cloud top properties of typhoon "Lupit" can be shown in the Fig. 3 as a preview of the POLDER3 level 2 product. The CALIPSO current algorithm is different from the earlier versions, so we need to think about the observation time of the CALIPSO products. Considering that these products were observed in 2009, so we should refer to the version 2.4 of CALIPSO data catalog released by NASA in 2007. In this version, cloud phase is determined by depolarization and backscattering correlation and combined temperature and backscattering threshold.

According to the DSOF algorithm, we first preprocessed the laser, microwave, and polarization data respectively. The CALIPSO data have a relative high resolution than other data. The information of cloud phase is recorded in the VFM. According to the phase of CALIPSO level 2 products, we find there is the same meaning to 0 and 1, and the different meanings to 2 and 3 by comparing the numerical value of CloudSat. Therefore, we unify cloud phase mask (Table 1). According to the longitude and latitude of CALIPSO level 2 products, the corresponding MODIS cloud phase is extracted, and the phase format is unified to the defined mode. Similarly, there are great differences in the representation of POLDER3 cloud phase values, so it necessary to simplify the POLDER3 cloud phase data with 0–99 changed to 3, 100–199 changed to 1, 200–229 changed to 2, and others changed to 0 (see POLDER3-simple in Table 1).

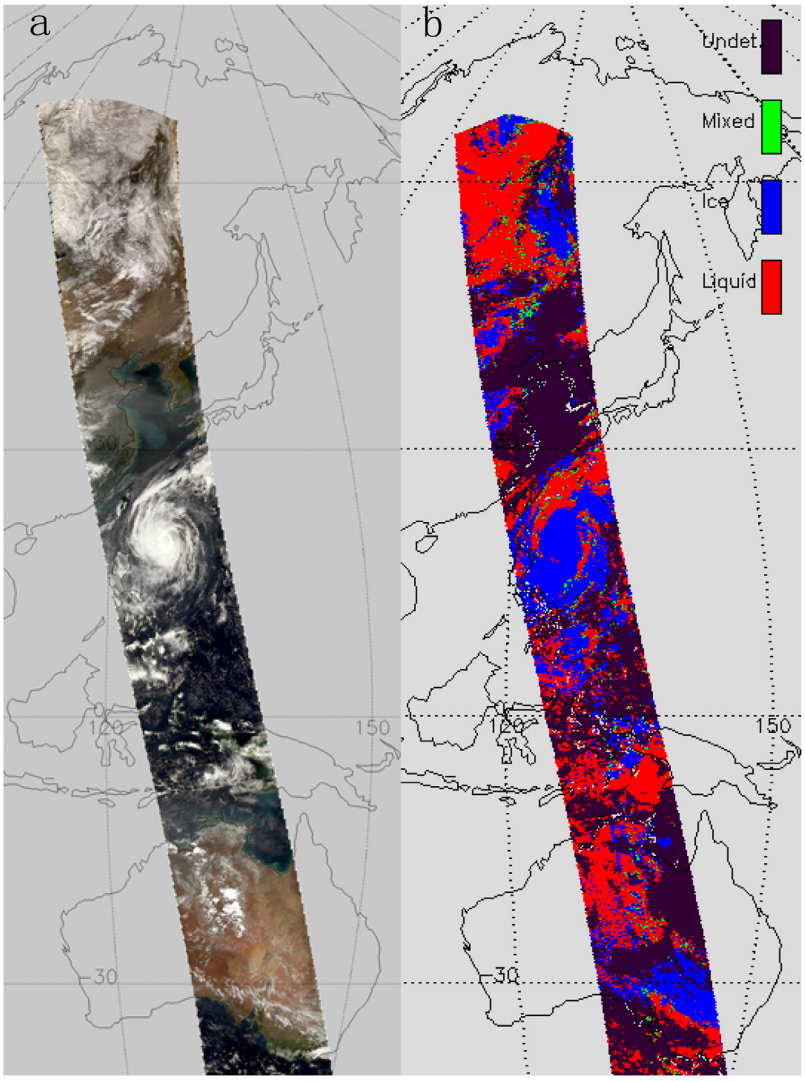

Fig. 3. Preview of POLDER3 product passed through the Typhoon "Lupit" (21 October 2009). (a) True color composite, (b) CTP of POLDER3.

Table 1
The cloud phase classification of different methods.

Number	CALIPSO	CloudSat	POLDER3-simple	MODIS	Unify
0	Unknown	Undetected	Unknown	Cloud-free	Unknown
1	Ice phase	Ice phase	Ice phase	Water phase	Ice phase
2	Water phase	Mixed phase	Mixed phase	Ice phase	Mixed phase
3	Mixed phase	Water phase	Water phase	Mixed phase	Water phase

Then we unify the expression of POLDER3 cloud phase (0 is unknown or undetermined, 1 is ice phase, 2 is mixed phase, 3 is water phase). This uniform cloud phase value is defined as a standard fusion phase representation.

After all products of four sensors are processed, we will get the new CTP using the DSOF algorithm. We read cloud phase values from VFM and 2B-CLDCLASS-LIDAR respectively. The CTP is obtained by making projection transformation from the vertical profile data of CALIPSO, and the same to CloudSat. We take the CALIPSO's latitude and longitude as the reference standard. Then the CTP of CloudSat, PARASOL, and MODIS are acquired by the nearest search with the matching reference location. Using the DSOF algorithm the fusion CTP can be obtained from POLDER3, CloudSat, and CALIPSO products. After that, the optimal fusion CTP are processed by the DSOF method (shown in Fig. 4).

Fig. 4 shows the latitude is limited to 0°−30° on the basis of CALIPSO data, and the longitude is limited to 131.2°−124.4° Taking the latitude 0°−30° as restrictive condition, the nearest search method is used to obtain the value of other sensors corresponding to the latitude and longitude of CALIPSO. The number 0 of CTP is the unknown or undetermined clouds, 1 is ice phase clouds, 2 is mixed phase clouds, and 3 is water phase clouds. The purple dots are the CALIPSO CTP algorithm (Fig. 4a), the blue dots are the CloudSat CTP algorithm (Fig. 4b), the orange scatter dots are the POLDER3 CTP algorithm (Fig. 4c), and the green dots are the MODIS CTP algorithm (Fig. 4d). The red dots are the Fusion CTP of

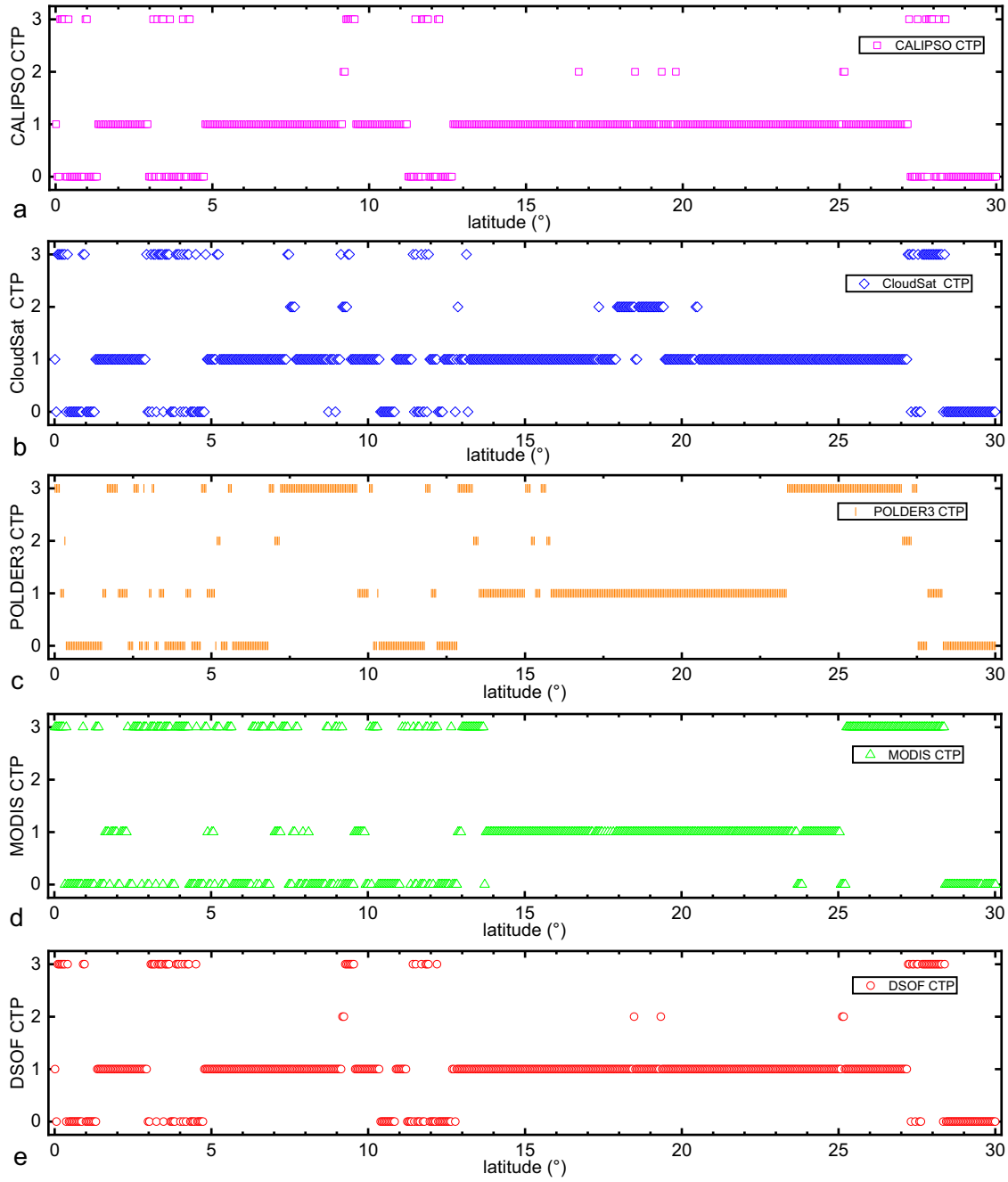

Fig. 4. Cloud phase of different sensors and methods passed through Typhoon "Lupit" with latitude from 0° to 30° (a) the CTP of CALIPSO, (b) the CTP of CloudSat, (c) the CTP of POLDER3, (d) the CTP of MODIS, and (e) the DSOF CTP of POLDER3, CloudSat, and CALIPSO.

CALIPSO, CloudSat, and POLDER3, which is computed by the DSOF method (Fig. 4e).

According to Fig. 4, we calculate the proportion of cloud phase obtained by different algorithms, and we also get a fusion ratio by using the optimal rules established in Section 3. These results of cloud phase are shown in Table 2 based on DSOF rule. When three phase is not the same, the coefficients are changeable. Through statistical analysis, we find that when all the coefficients take 1/3, the fusion ratios are optimal. From the Table 2, we find the ratio of water cloud by DSOF method is significantly smaller than that of CALIPSO, CloudSat and PARASOL. However, the ratio of unknown/water clouds by DSOF method is more close to that of CloudSat, and the ratio of ice/mixed phase clouds is more close to that of CALIPSO.

5. Discussion

From Table 2, it can be seen that there is a little difference in the cloud proportion of active sensors CALIPSO and CloudSat, and the ratio of unknown and undetermined area is 19.7% and 16.3%, respectively, ice cloud's ratio is 73.2% and 67.6%, mixed cloud's ratio is 1.2% and 6.6% respectively, water cloud's ratio is 5.8% and 9.6%. By comparing the CALIPSO and CloudSat data, we know that the ice cloud's ratio is slightly lower, and the ratio of the undetermined and clear area also decreased slightly, and the ratio of water clouds and mixed clouds have increased. The reason for the above changes is that the millimeter wave can penetrate most ice particles, and the radar can obtain the reflection energy of most liquid droplets of the vertical profile. Similarly, the CloudSat cloud phase

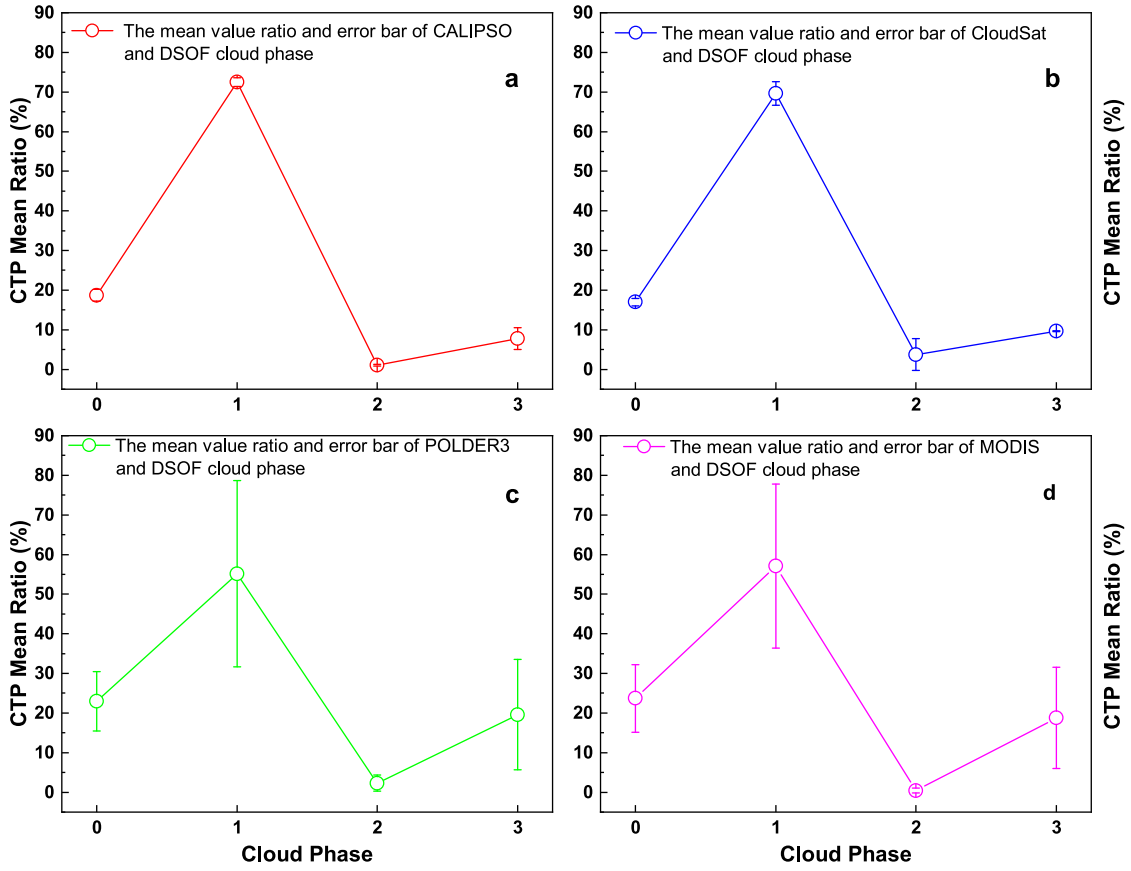

Fig. 5. The CTP mean value ratio and error bar of typhoon area is counted by comparing DSOF method with others, the X-axis represents cloud phase classification, 0 is the unknown or undetermined, 1 is ice phase, 2 is mixed phase, 3 is water phase, and the Y-axis is CTP mean ratio.

Table 2
The ratio of cloud phase computed by different algorithm.

Algorithm	*a*	*b*	*c*	Rule	Unknown ratio	Ice phase ratio	Mixed phase ratio	Water phase ratio
CALIPSO	1	0	0	–	19.7%	73.2%	1.2%	5.8%
CloudSat	0	1	0	–	16.3%	67.6%	6.6%	9.6%
PARASOL	0	0	1	–	28.3%	38.6%	3.7%	29.4%
MODIS	–	–	–	–	29.7%	42.5%	0	27.8%
DSOF	1/3	1/3	1/3	DSOF	17.6%	71.7%	0.9%	9.7%

inversion combined with CALIPSO laser radar backscatter information makes the detecting accuracy of cloud top ice particles had not been greatly reduced.

From Table 2, we can see that the cloud phase classification ratios of passive sensor POLDER3 and MODIS are close, and the ratio of the unknown and undetermined area is 28.3% and 29.8%, respectively. The ratio of ice clouds is 38.6% and 42.5%. The ratio of mix clouds is 3.7% and 0% (because MODIS's latest product is no longer producing mixed cloud data). The ratio of water clouds is 29.5% and 27.8%, respectively. The ratio of ice clouds decreased significantly, and the water clouds and undetected and clear sky area increased significantly. Because the resolution of POLDER3 and MODIS is low, and the detection of thin clouds and broken clouds are not very good. Especially there are transparent clouds above thick clouds and multilayer clouds. In POLDER3 multi-angle observation, it is easy to detect this part of clouds, so that the cloud phase identification can penetrate the transparent part of cloud top to reach the interior, thus identifying the internal water phase as the top water clouds. Similarly, MODIS mainly uses the infrared brightness temperature method to recognize cloud phase, and this method is not sensitive to the temperature of thin cloud top and base, and cannot identify transparent thin clouds. The proportion of cloud phase obtained by DSOF is also shown in Table 2, the ratio of unknown and undetermined regions is 17.6%, the ratio of ice clouds is 71.7%, the ratio of mix phase clouds is 0.9%, and the ratio of water clouds is 9.7%. We compared the CTP ratio of DSOF with the results obtained by the other four methods, and the mean value ratio and error bar is shown in Fig. 5. The CTP mean ratio of CALIPSO and DSOF is 18.7%, 72.5%, 1.0% and 7.8%. The CTP mean ratio of CloudSat and DSOF is 17.0%, 69.7%, 3.7% and 9.6%. The CTP mean ratio of POLDER3 and DSOF is 22.9%, 55.2%, 2.3% and 19.6%. The CTP mean ratio of MODIS and DSOF is 23.7%, 57.1%, 0.4% and 18.8%. From Fig. 5a-d, we find the error bars are relatively short in Fig. 5a and Fig. 5b, at the same time the error bars are longer in Fig. 5c and Fig. 5d. The main reason for this difference is that the resolution of CALIOP and CPR is higher than that of POLDER3 and MODIS, and the lasers and millimeter waves can detect the particle phase in the top and inside of the cloud. The POLDER3 and MODIS sensors cannot effectively obtain the reflection information of thin and broken clouds.

The standard deviation RSE_x of the cloud phase of different algorithms and the fusion cloud phase is calculated. The calculation

formula is as follows:

$$\mathrm{RSE}_x = \sqrt{\sum \left(Ratio_x^i - Ratio_{Fusion}^i\right)^2} \quad (4)$$

where i is the type of cloud phase ($i = 0, 1, 2, 3$), and x is the cloud phase identification of different sensors, and *Ratio* is the proportion of different cloud phase in the cloud layer.

We calculated the standard deviations between the results of DSOF CTP and other methods. The RSE of CALISPO is 4.67%, the RSE of CloudSat is 7.18%, the RSE of POLDER3 is 40.14%, and the RSE value of MODIS is 36.51%. It can be seen that the fusion method is very different from the passive sensors, which is close to the value of the active sensors and is closest to the CALISPO CTP. This method can effectively reduce the range of undetected area and mixed clouds, and effectively improve the detection efficiency of water clouds and accuracy of ice clouds.

6. Conclusions

The level 2 products of the typhoon “Lupit” were observed by four satellites of CALIPSO, CloudSat, POLDER3, and MODIS. The descending dimension of multidimensional space is carried out. Under the same resolution, the spatial fusion of three sensors (CALIPSO, CloudSat, and POLDER3) is realized by using the DSOF method. Comparing the fused cloud phase with the other four sensors, it is found that this method has obvious advantages in identifying CTP, and its recognition effect is closer to cloud phase products of laser sensor (CALIPSO), and the proportion of mixed clouds are reduced about 0.3%. Compared with MODIS, the fusion results of CTP showed that this method can greatly improve the recognition accuracy of thin and transparent clouds, and reduce the ratio of water clouds and undetected and clear-sky area.

The traditional cloud phase inversion mainly focuses on single sensor or single direction, and the multi-sensor inversion is relatively limited. The data that satisfies the collaborative processing is relatively small. Space cooperative inversions of multi-sensor need the consistent orbit height and synchronous observing condition. In this paper, a combined algorithm of multidimensional spatial data is constructed by combining active and passive sensors, especially the combination of three sensors (POLDER3, CALIPSO, and CloudSat), so as to achieve the spatial synergy of cloud phase. This method is a new attempt for CTP fusion, and we find that this fusion result is close to the active sensors at a time of minimal change in the cloud system. Furthermore, it has the following significance for the cloud phase recognition of different sensors at present. It can extend the range of the data and supplements the high precision data. Additionally, the synergistic inversion can not only greatly improve the retrieval accuracy of cloud phase, but also provide new technology for cloud microphysical characteristic inversion and a new solution for the development of multi-sensor satellite.

Acknowledgment

This research is partially supported by the Key Project of Hefei Institutes of Physical Sciences of Chinese Academy of Sciences, the Major Project of High Resolution Earth Observation System (32-Y20A22-9001-15/17), and the Project of Chinese satellite resource center. The authors gratefully acknowledge the ICARE Data and Services Center of Lille-1 University for providing the POLDER3 products, the Atmospheric Science Data Center (ASDC) of NASA Langley Distributed Active Archive Center (DAAC) for providing the CALIPSO products, the CloudSat Data Processing Center of Colorado University for providing CloudSat products, the NASA Earth Observing System and Information System for providing the MODIS products. We thank Space Research Software LLC for providing the HDF Explorer tool. We also gratefully acknowledge the anonymous reviewers for their time and effort in helping us improve the manuscript.

Supplementary materials

Supplementary material associated with this article can be found, in the online version, at doi:10.1016/j.jqsrt.2018.11.010.

References

[1] Liou KN. Influence of cirrus clouds on weather and climate processes: a global perspective. Mon Wea Rev 1986;114:1167–99.
[2] Stephens GL, Tsay SC, Stackhouse PW, Flatau PJ. The relevance of the microphysical and radiative properties of cirrus clouds to climate and climatic feedback. J Atmos Sci 1990;47:1742–53 https://doi.org/10.1175/1520-0469(1990)047⟨1742:trotma⟩2.0.co;2.
[3] Riédi J. Laboratoire d'Optique Atmosphérique Analysis of cloud thermodynamic phase at global scale using polarimetric multiangle measurements from the POLDER1/ADEOS1, Ph.D. thesis. Universitédes Sciences et Technologies de Lille; 2001.
[4] Hutchison KD, Etherton BJ, Topping PC, Huang HL. Cloud top phase determination from the fusion of signatures in daytime AVHRR imagery and HIRS data. Int J Remote Sens 1997;18:3245–62. https://doi.org/10.1080/014311697217062.
[5] Knap W, Stammes P, Koelemeijer RB. Cloud thermodynamic phase determination from near-infrared spectra of reflected sunlight. J Atmos Sci 2002;59:83–96.
[6] Key J, Intrieri J. Cloud particle phase determination with the AVHRR. J Appl Meteorol 2000;39:1797–805. https://doi.org/10.1175/1520-0450-39.10.1797.
[7] Platnick S, King MD, Ackerman SA, Menzel WP, Baum BA, Riedi J, Frey RA. The MODIS cloud products: algorithms and examples from Terra. IEEE Trans Geosci Remote Sens 2003;41:459–73. https://doi.org/10.1109/tgrs.2002.808301.
[8] Ackerman SA, Smith WL, Revercomb HE, Spinhirne JD. The 27-28 October 1986 FIRE IFO cirrus case study. Spectral properties of cirrus clouds in the 8–12 μm window. Mon Wea Rev 1990;118:2377–88. https://doi.org/10.1175/1520-0493(1990)118⟨2377:toficc⟩2.0.co;2.
[9] Strabala KI, Ackerman SA, Menzel WP. Cloud properties inferred from 8–12 μm data. J Appl Meteorol Climatol 1994;33:212–29.
[10] Baum BA, Soulen PF, Strabala KI, King MD, Ackerman SA, Menzel WP, et al. Remote sensing of cloud properties using MODIS airborne simulator imagery during SUCCESS II. Cloud thermodynamic phase. J Geophys Res 2000;105:11781–92. https://doi.org/10.1029/1999jd901090.
[11] Rossow WB, Schiffer RA. Advances in understanding clouds from ISCCP. Bull Amer Meteor Soc 1999;80:2261–87 https://doi.org/10.1175/1520-0477(1999)080⟨2261:aiucfi⟩2.0.co;2.
[12] King MD, Plantnick S, Yang P, Arnold GT, Gray MA, Riedi JC, et al. Remote sensing of liquid water and ice cloud optical thickness and effective radius in Arctic: application of airborne multispectral MAS data. J Atmos Ocean Technol 2004;21:857–75.
[13] Goloub P, Herman M, Chepfer H, Riédi J, Brogniez G, Couvert P, et al. Cloud thermodynamic phase classification from the POLDER spaceborne instrument. J Geophys Res 2000;105:14747–59. https://doi.org/10.1029/1999jd901183.
[14] Riédi J, Marchant B, Platnick S, Baum BA, Thieuleux F, Oudard C, et al. Cloud thermodynamic phase inferred from merged POLDER and MODIS data. Atmos Chem Phys 2010;10:11851–65. https://doi.org/10.5194/acp-10-11851-2010.
[15] Hu Y, Winker D, Vaughan M, Lin B, Omar A, Trepte C, et al. CALIPSO/CALIOP cloud phase discrimination algorithm. J Atmos Ocean Technol 2009;26:2293–309.
[16] Wang Z, Sassen K. Cloud type and macrophysical property retrieval using multiple remote sensors. J Appl Meteorol Climatol 2001;40:1665–82.
[17] Cho HM, Nasiri SL, Yang P. Application of CALIOP measurements to the evaluation of cloud phase derived from MODIS infrared channels. J Appl Meteorol Climatol 2009;48:2169–80. https://doi.org/10.1175/2009jamc2238.1.
[18] Deschamps PY, Bréon FM, Leroy M, Podaire A, Bricaud A, Buriez JC, et al. The POLDER mission: instrument characteristics and scientific objectives. IEEE Trans Geosc Rem Sens 1994;32:598–615. https://doi.org/10.1109/36.297978.
[19] Parol P, Buriez JC, Vanbauce C, Riedi J, Labonnote LC, Doutriaux-Boucher M, et al. Review of capabilities of multi-angle and polarization cloud measurements from POLDER. Advan Space Res 2004;33:1080–8. https://doi.org/10.1016/s0273-1177(03)00734-8.
[20] Li Z, Goloub P, Devaux C, Gu X, Deuzé JL, Qiao Y, et al. Retrieval of aerosol optical and physical properties from ground-based spectral, multi-angular and polarized sun-photometer measurements. Remote Sens Environ 2006;101:519–33. https://doi.org/10.1016/j.rse.2006.01.012.
[21] Dubovik O, Herman M, Holdak A, Lapyonok T, Tanré D, Deuzé JL, et al. Statistically optimized inversion algorithm for enhanced retrieval of aerosol properties from spectral multi-angle polarimetric satellite observations. Atmos Meas Tech 2010;3:4967–5077. https://doi.org/10.5194/amtd-3-4967-2010.
[22] Chepfer H, Goloub P, Riedi J, De Haan JF, Hovenier JW, Flamant PH. Ice crystal shapes in cirrus clouds derived from POLDER-1/ADEOS-1. J Geophys Res 2001;106:7955–66. https://doi.org/10.1029/2000jd900285.
[23] Riédi J, Goloub P, Marchand RT. Comparison of POLDER cloud phase retrievals to active remote sensors measurements at the ARM SGP site. Geophys Res Lett 2001;28:2185–8. https://doi.org/10.1029/2000gl012758.

[24] Bréon FM, Goloub P. Cloud droplet effective radius from spaceborne polarization measurements. Geophys Res Lett 1998;25:1879–82. https://doi.org/10.1029/98gl01221.
[25] Sassen K. The polarization lidar technique for cloud research: a review and current assessment. Bull Amer Meteor Soc 1991;72:1848–66.
[26] Hu Y, Winker D, Yang P, Baum B, Poole L, Vann L. Identification of cloud phase from PICASSO-CENA lidar depolarization: a multiple scattering sensitivity study. J Quant Spectrosc Radiat Transfer 2001;70:569–79. https://doi.org/10.1016/s0022-4073(01)00030-9.
[27] Hu Y. Depolarization ratio-effective lidar ratio relation: theoretical basis for space lidar cloud phase discrimination. Geophys Res Lett 2007;34:L11812. https://doi.org/10.1029/2007gl029584.
[28] Stephens GL, Vane DG, Boain RJ, Mace GG, Sassen K, Wang Z, et al. The CloudSat mission and the A-Train: a new dimension of space-based observations of clouds and precipitation. Bull Amer Meteoro Soc 2002;83:1771–90. https://doi.org/10.1175/bams-83-12-1771.
[29] Mischenko M, Travis L, Lacis A. Multiple scattering of light by particles. New York, Cambridge: Cambridge University Press; 2006.
[30] Nasiri SL, Kahn BH. Limitations of bi-spectral infrared cloud phase determination and potential for improvement. J Appl Meteorol Clim 2008;47:2895–910. https://doi.org/10.1175/2008jamc1879.1.
[31] Lay DC. Linear algebra and its applications. 2nd edition. New York: Addison-Wesley; 2000.